Hindawi
Journal of Nanomaterials
Volume 2022, Article ID 8961362, 8 pages
https://doi.org/10.1155/2022/8961362

Research Article

Silica Nanoparticle Coating of $NaYF_4$:(Yb^{3+}, Er^{3+}) Upconversion Phosphor

Taehun Jang, MaengJun Kim, and Sang Ho Sohn

Department of Physics, Kyungpook National University, Daegu 41566, Republic of Korea

Correspondence should be addressed to Sang Ho Sohn; shsohn@knu.ac.kr

Received 25 March 2022; Revised 24 May 2022; Accepted 8 July 2022; Published 28 July 2022

Academic Editor: N Senthilkumar

To improve its light conversion efficiency, $NaYF_4$:(Yb^{3+}, Er^{3+}) upconversion (UC) phosphor, which generates one visible photon by absorbing two or more near-infrared photons, was coated with SiO_2 nanoparticles. The surface modification of phosphor was performed by using a modified sol–gel method as a function of the concentration of colloidal silica employed as the surface coating precursor. It was found that the PL intensities depend on the concentration of colloidal silica. When a 2.7 wt% concentration of colloidal silica was used, the $NaYF_4$:(Yb^{3+}, Er^{3+}) phosphor exhibited a homogeneous coating with silica and an approximately 9% increase in the PL intensity, as compared with that of the non-coated sample of $NaYF_4$:(Yb^{3+}, Er^{3+}) phosphor. This increase in the PL intensity can be explained by the suppression of the nonradiative recombination of electron–hole pairs via surface defects. The experimental results suggest that the surface modification of upconversion phosphors with a silica coating of the appropriate concentration is a simple and effective solution to improve the light conversion efficiency of upconversion phosphors used in optoelectronic devices.

1. Introduction

Thus far, hexagonal $NaYF_4$ nanocrystals with sizes in the 20–30 nm range have been the most efficient host materials for green and blue upconversion (UC) phosphors exhibiting visible emission by IR excitation [1]. In the host material, Y^{3+} can be replaced at any ratio by the rare earth ions Yb^{3+} and Er^{3+} for green UC phosphors. Meanwhile, significant research has been accomplished to improve the material properties of lanthanide-doped upconversion nanoparticles (UCNPs), particularly the quantum yield (QY) of solar cells and biochips. Among such research, studies on the influence of shelling with meso- and microporous silica on fluorescence characteristics are notable examples [1, 2].

Figure 1 depicts the UC processes of Er^{3+} and Yb^{3+} codoped $NaYF_4$ phosphors. The main absorption process of Yb^{3+} is the $2F_{7/2} \rightarrow 2F_{5/2}$ transition at 980 nm [3]. The most dominant excitation path in Er^{3+} is $4I_{15/2} \longrightarrow 4I_{11/2} \longrightarrow 4F\ 7/2$, which requires two energy transfers for the $2F_{7/2} \longrightarrow 2F_{5/2}$ transition of Yb^{3+}. Subsequent multiphonon relaxation populates the emitting $2H_{11/2}$ and $4S_{3/2}$ states. Through further excitation and cross-relaxation processes, the populations of the $2H_{9/2}$ and $4F_{5/2}$ states were also obtained [4, 5]. A previous study using a delicate photoluminescence measurement reported that the QY of UCNPs was lower than 0.3% for the green emission in NaYF4:(Er^{3+}, Yb^{3+}) UCNP phosphors, whereas a QY of 3% was measured for an upconversion microparticle (UCMP) phosphor [6]. Despite extensive research [1, 2, 7–10], satisfactory QYs have seldom been obtained. Therefore, the QY of UCNPs should be improved using a specific method. UCNP phosphors exhibit a larger surface area/bulk volume ratio than UCMP phosphors. The surfaces of the phosphors exhibit inevitable surface defects that are formed when they are synthesized. Therefore, the surface defect density per unit volume of UCNP phosphors can be larger than that of UCMP phosphors. It is well known that nonradiative decay can occur via the surface defects of emissive materials. This could explain why the QY of the UCNP phosphors is significantly lower than that of the UCMP phosphors. It is of interest that research based on the energy transfer mechanism [3, 11] for

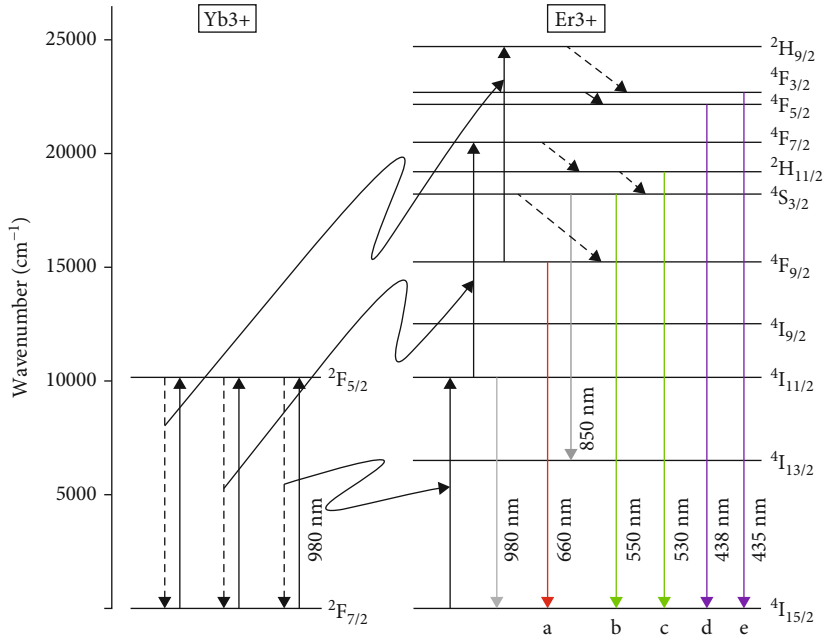

Figure 1: UC processes in Er^{3+} and Yb^{3+} codoped $NaYF_4$ phosphors.

the improvement of the QY of UCMP phosphors has been accomplished. From the viewpoint of the QY, UCMP phosphors are more promising than UCNP phosphors.

Earlier studies [12–14] related to the surface modification of microphosphors have suggested that surface coating with oxides is an important technique for improving phosphor characteristics, such as luminance. The present study is aimed at substantiating the same and suggests a silica nanoparticle coating on the surface of the UCMP phosphors. To obtain nanoparticle-coated UCMP phosphors with improved luminance performance, we prepared NaYF4:(Yb^{3+}, Er^{3+}) microphosphors coated with SiO_2 nanoparticles using a modified sol–gel method and investigated their optical properties. The modified sol–gel method used for surface treatment in this work is a simple and low-temperature (below 100°C) process, as compared with other chemical methods [15].

2. Materials and Methods

Commercially available hexagonal NaYF4:(Yb^{3+}, Er^{3+}) (18% and 2% doped, respectively) microphosphor (KPT 980 nm, Shanghai Keyan Phosphor Technology Co., Ltd.) was coated with SiO_2 using a modified sol–gel method in which colloidal silica (LUDOX-AM-30; Sigma-Aldrich Chemicals Pvt., Ltd.) with an average particle size of 12 nm was employed as a precursor. As reported in our earlier studies [12, 13], the SiO_2-coated phosphors were obtained as follows: (1) Various concentrations of colloidal SiO_2 nanoparticles were prepared by dilution using deionized (DI) water. (2) 10 g of NaYF4:(Yb^{3+}, Er^{3+}) was added to 100 ml of diluted colloidal SiO_2 with continuous stirring using a magnetic bar for 3 h. (3) The resulting phosphor suspensions were washed twice with DI water. (4) SiO_2-coated phosphors were obtained by filtering and drying the washed phosphor suspension at 80°C for 12 h. The morphological properties of the coated and the noncoated UC phosphors were compared using a scanning electron microscope (SEM). To perform surface analysis, an X-ray photoelectron spectroscopy (XPS) system (ULVAC-PHI Quantera SXM) equipped with a monochromated Al Kα source and a hemispherical analyzer was used. The energy resolution of the XPS system for high-resolution core-line scans was set to 0.1 eV. The spot size was set to 0.4 mm.

As shown in Figure 2, a PL measurement system was set up to determine the UC efficiencies of the phosphor samples. A simple IR laser diode with a wavelength of 980 nm was used for excitation. An equal amount of phosphor powder was placed in a quartz cuvette. The laser and quartz cuvettes were reproducibly positioned on an optical table. The optical spectrum was acquired by configuring instruments manufactured by EG&G Princeton Applied Research. All measurements were performed at room temperature. The emitted light was coupled into a fixed optical fiber and measured in the 384–716 nm range using a zzodel 1237 dual-port optical modulation amplitude (OMA) spectrograph with a Model 1420 photodiode array (PDA). The metal pipe holder is used to fix the optical fiber. The electrical signal acquisition was performed using a Model 1461 detector interface.

3. Results and Discussion

Figure 3 presents the SEM images of the $NaYF_4$:(Yb^{3+}, Er^{3+}) phosphors coated with nanoparticles at several colloidal silica concentrations and the noncoated phosphors. The size of the non-coated UC phosphor was in the 1–10 μm range, as shown in Figure 3(a). As shown with dotted circles in Figures 3(b)–3(e), it can be easily observed that the surfaces of the $NaYF_4$:(Yb^{3+}, Er^{3+}) phosphors are covered with fine

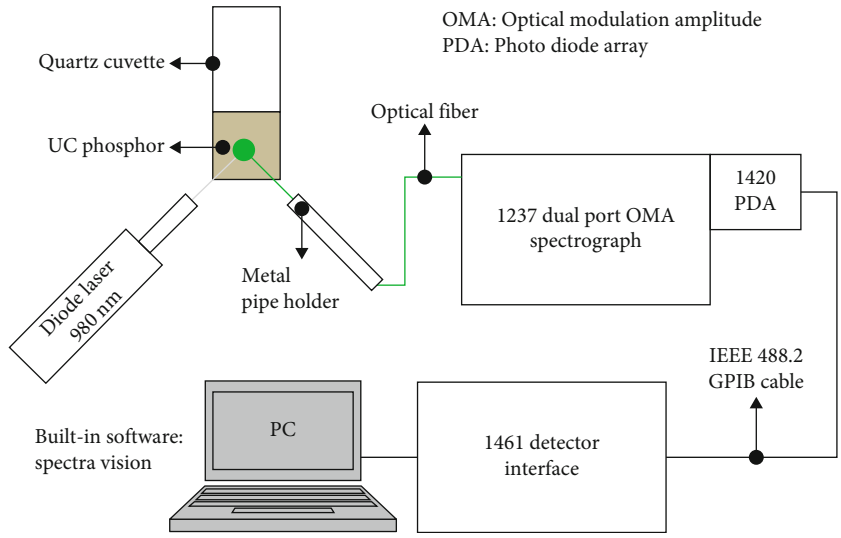

Figure 2: PL measurement system for the UC efficiencies of the phosphor samples.

nanoparticles featuring a size of ~100 nm. As expected, it was observed that the silica concentration significantly affected the surface morphology of the UC phosphors. For the 0.3 wt% and 1.5 wt% concentrations, the coverage of nanoparticles was insufficient to coat the UC phosphors homogeneously, as shown in Figures 3(b) and 3(c). For the 2.7 wt% condition, a homogeneous coating was obtained, as shown in Figure 3(d). For all higher mole concentrations such as 5.0 wt%, the uniformity of the coating on the UC phosphors was observed to deteriorate, exhibiting a type of cluster. As shown in Figure 3(e), the existence of large clusters of nanoparticles implies that, before adhesion to the surface of the UC phosphors, the nanoparticles aggregate and then couple with the UC phosphors. However, at this point, it was difficult to confirm whether the fine nanoparticles in the SEM images were SiO_2 nanoparticles. For this purpose, surface analysis, such as XPS, was required.

Figure 4 shows the XPS spectra of the respective elements of the $NaYF_4$:(Yb^{3+}, Er^{3+}) phosphor, with respect to the SiO_2 concentrations. Figures 4(a)–4(f) illustrate the survey scan, Si 2p, O 1s, Na 1s, Y 3d, and F 1s XPS spectra, respectively. In Figure 4(a), to compare between the relative XPS peak intensity, only peaks for silica concentration of 2.7 wt% are introduced because we could not draw all peaks for five silica concentrations in a graph without overlapping. The survey scan spectrum reveals the presence of Si, O, Na, Y, and F elements. As shown in Figure 4(b), Si peaks were observed only in the SiO_2-coated phosphor, unlike the non-coated phosphor (0 wt%). From the NIST Standard Reference Database 20, it is found that Si 2p peak shown in Figure 4(b) originates from the convolution of the peaks related to the Si-O bonds. In addition, as exhibited in Figure 4(c), strong O peaks are observed in the SiO_2-coated phosphor, compared to the noncoated phosphor (0 wt%). The weak O peaks observed in the non-coated phosphor are probably related to the presence of residual oxygen in the $NaYF_4$:(Yb^{3+}, Er^{3+}) phosphor, which is an intrinsic impurity. Thus, the presence of SiO_2 nanoparticles covering the $NaYF_4$:(Yb^{3+}, Er^{3+}) phosphors can be confirmed by the Si 2p and O 1s spectra. Further, it can be confirmed that the nanosized particles observed in Figure 3 are composed of SiO_2. In addition, as expected, it was observed that the Na- and F-related peaks decreased to a large extent after silica coating. It should be noted that, for all the samples coated with SiO_2 nanoparticles, the Na 1s, Y 3d, and F 1s peaks yield slight shifts (0.2–0.3 eV) to higher binding energies, as compared with those for the noncoated phosphor. This suggests that the residual NaF compound affects the chemical binding energy of the respective elements of the $NaYF_4$ host crystal, causing a small shift to lower binding energies in the case of the noncoated $NaYF_4$:(Yb^{3+}, Er^{3+}) phosphor. To the best of our knowledge, no references for any elements consisting of $NaYF_4$ have been registered in scientific databases. However, a similar stoichiometric compound such as sodium fluoroborate ($NaBF_4$) can provide a reasonable explanation. According to the NIST Standard Reference Database 20, version 3.5, for NaF, the Na 1s and F 1s reference peaks are observed at 1071.2 eV and 684.5 eV, respectively. However, for $NaBF_4$, the Na 1s and F 1s reference peaks appear at 1072.7 eV and 687 eV, respectively. Thus, it is suggested that these shifts are due to the absence of NaF. These results are consistent with the XPS results described above. In addition, Y 3d peaks shown in Figure 4(e) have well-resolved spin-orbit components corresponding to the total angular momentum $J = 3/2$, and $J = 5/2$ states. The peak observed in the vicinity of 153 eV in Figure 4(e) is associated with Si 2s.

Figure 5(a) shows the PL spectra in the visible region for the $NaYF_4$:(Yb^{3+}, Er^{3+}) phosphors coated with silica at several concentrations. In Figure 5(a), the main emission wavelength regions labeled A, B, C, D, and E are associated with the emission transitions shown in the energy-level diagrams depicted in Figure 1. For clarity, enlarged figures of the specific wavelength ranges in Figure 5(a) are also shown in Figures 5(b)–5(e). For all the wavelengths in the emission spectrum shown in Figure 5(a), the integrated area was

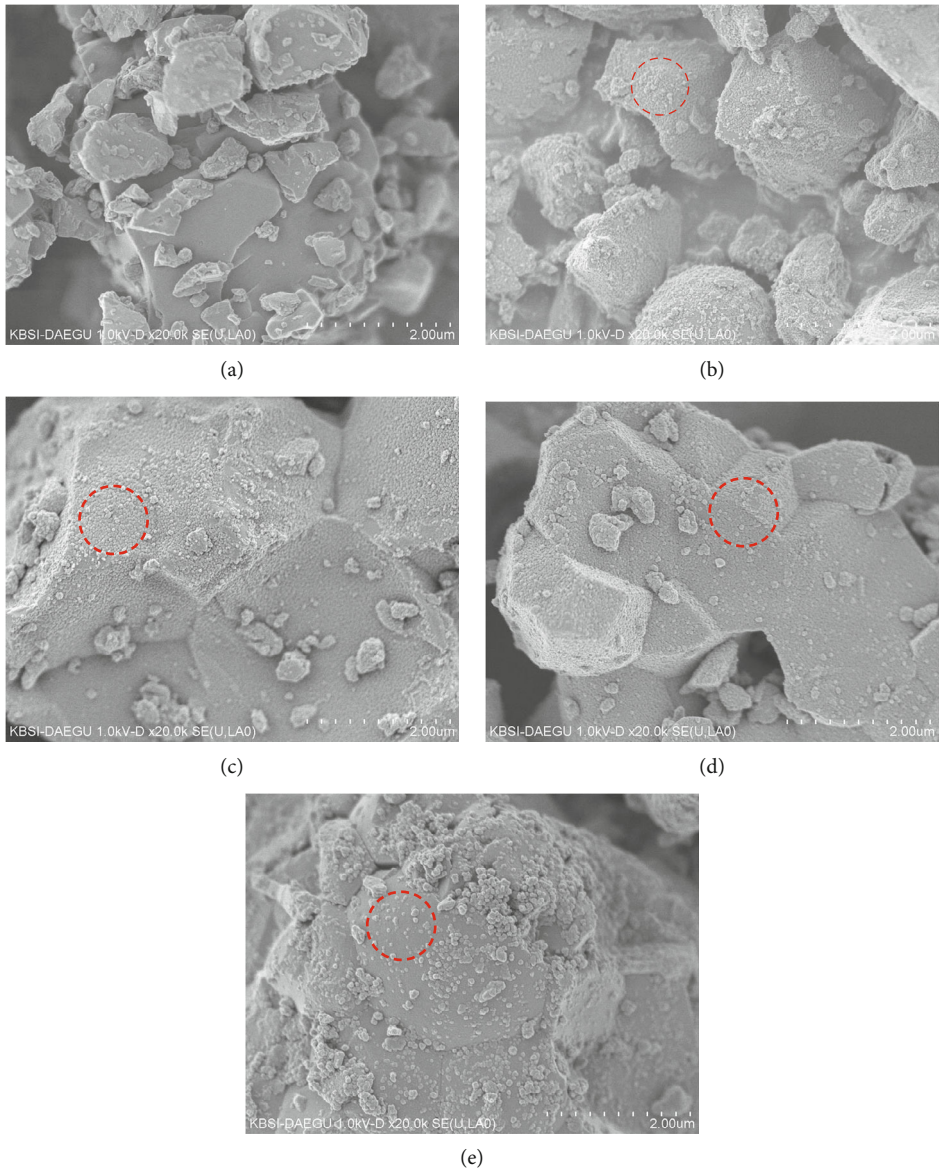

Figure 3: SEM images of $NaYF_4$:(Yb^{3+}, Er^{3+}) phosphors coated with nanoparticles at several colloidal silica concentrations and noncoated phosphor ((a) noncoated 0 wt%, (b) 0.3 wt%, (c) 1.4 wt%, (d) 2.7 wt%, and (e) 5.0 wt%). The dotted circles represent nanoparticles coated on the surface of $NaYF_4$:(Yb^{3+}, Er^{3+}) microphosphors.

calculated to enable a quantitative comparison. The estimated calculation demonstrated that the intensities of the silica-coated phosphors at the 0.3 wt%, 1.4 wt%, and 2.7 wt% conditions were higher than those of the noncoated samples (0 wt%), without exhibiting any wavelength shifts in the core-level transition regions, thereby indicating that the presence of SiO_2 particles on the surface of the UC phosphors affects the PL intensity. For the 0.3 wt% and 1.4 wt% conditions, an increase of approximately 2% in the PL intensity was observed. The maximum PL performance was observed for the concentration of 2.7 wt%, whereby a PL characteristic improvement of approximately 9% was detected, as compared with that of the noncoated UC phosphors. These results suggest that the increase in the PL intensity is strongly related to the uniformity of the surface modification with oxides, as shown in Figures 3(b)–3(d). In contrast, for the 5 wt% condition, a decrease of almost 10% in the PL intensity of the coated phosphors was observed, as compared with that of the noncoated UC phosphors. These results can be easily analyzed based on the morphological properties acquired by the SEM measurements, as shown in Figure 4. As shown in Figure 3(e), a homogeneous nanoparticle coating is barely obtained. This was caused by the aggregation of SiO_2 nanoparticles, which hindered the impinging light from being absorbed by the phosphors and the emitted light from being transmitted. The influence of SiO_2 coating on the $NaYF_4$:(Yb^{3+}, Er^{3+}) UCNP has been reported in earlier research [1, 2, 15–18]. It is known that SiO_2 coating causes the $NaYF_4$:(Yb^{3+}, Er^{3+}) UCNP to protect UCNP from dissolution [1, 15], to improve the temperature

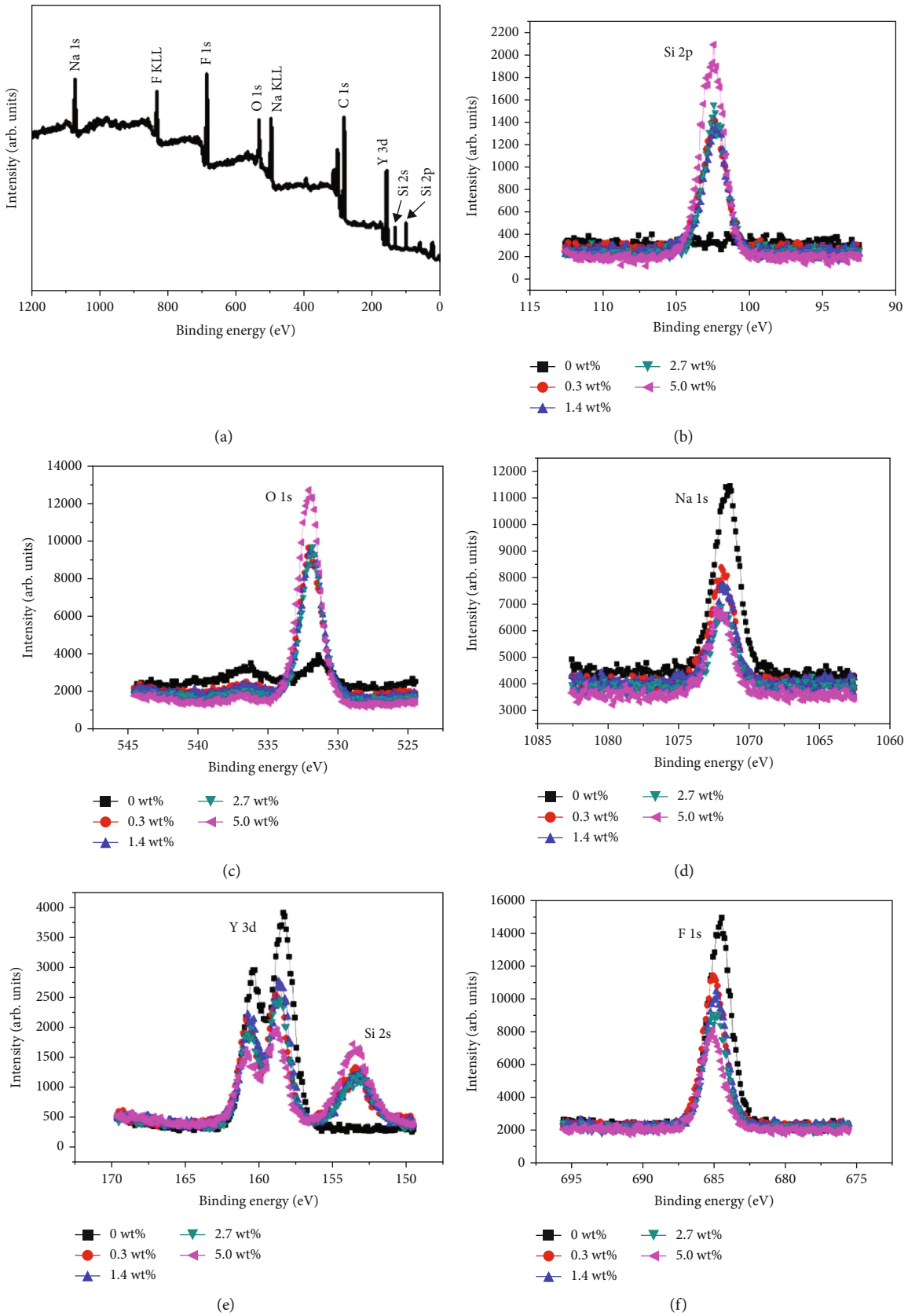

FIGURE 4: XPS spectra of the respective elements of $NaYF_4$:(Yb^{3+}, Er^{3+}) phosphor with respect to SiO_2 concentrations. (a) The survey scan, (b) Si 2p, (c) O 1s, (d) Na 1s, (e) Y 3d, and (f) F 1s XPS spectra.

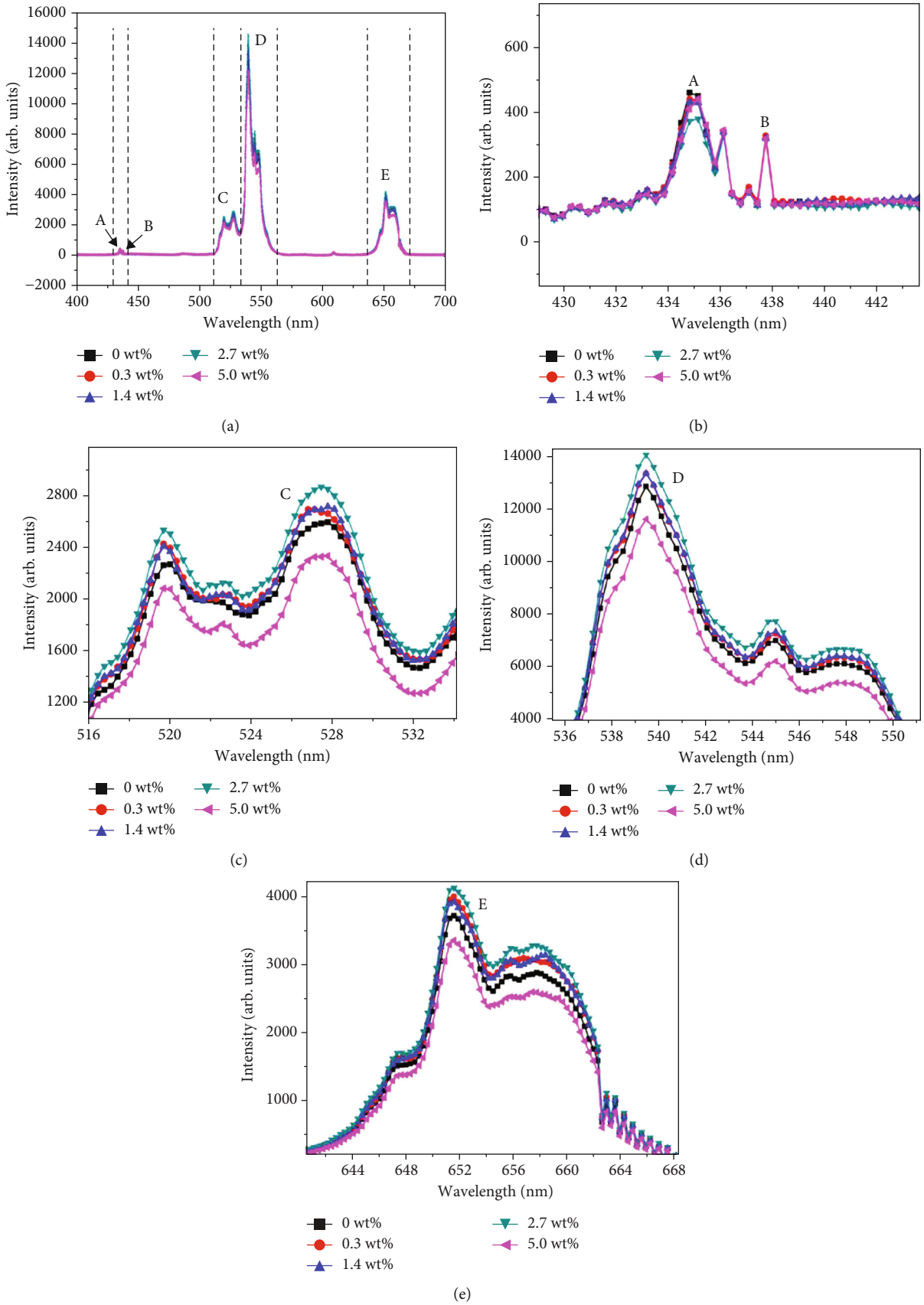

Figure 5: (a) PL spectra in the visible region for the $NaYF_4$:(Yb^{3+}, Er^{3+}) phosphors coated with SiO_2 at several concentrations. (b–e) Peaks denoted by A, B, C, D, and E in (a).

stability [2], to restore the chemical activity in aqueous media [16], to protect core from degradation in proteolytic solvents [17], and to enhance the adhesion of metal particles. But, as a whole, these studies report a decrease in PL intensities after SiO_2 coating on the $NaYF_4$:(Yb^{3+}, Er^{3+}) UCNP. The reason for it has not been argued in detail besides the light scattering effect on both emission and incident light by the SiO_2 layer. Meanwhile, it is known that SiO_2 @metal coating on the $NaYF_4$:(Yb^{3+}, Er^{3+}) UCNP results in an increase in the PL intensity by means of exciton–plasmon coupling, resulting from the metal coating [18].

Our samples consist of SiO_2 nanoparticles coated on upconversion microsized phosphors(UCMP), in contrast to those reported in earlier research [1, 2, 15–18]. Our $NaYF_4$:(Yb^{3+}, Er^{3+}) UCMP is not a nanoparticle but a bulky particle with lots of surface defects. Therefore, if SiO_2 coating reduces the surface defects, it is expected that the SiO_2 nanoparticles in our samples are a significant factor contributing toward the PL intensity, in contrast to the results reported in earlier studies [16]. Generally, radiation excites the bulky phosphor and generates free electron–hole pairs (e-h pairs). These e-h pairs diffuse into the surface defects and recombine nonradiatively, resulting in a decrease in the PL intensity [19]. SiO_2 nanoparticles coated on microsized phosphors could reduce surface defects and suppress the nonradiative recombination of e-h pairs via the surface defects, thus resulting in a higher PL intensity. Thus, the increase in the PL intensity due to the surface coating of the phosphors with oxide nanoparticles can be explained on the basis of the suppression of nonradiative recombination via surface defects, among the several other mechanisms discussed in an earlier study [13]. However, there is still no direct tangible evidence in favor of this mechanism in SiO_2-coated $NaYF_4$:(Yb^{3+}, Er^{3+}) microsystems. To achieve this, a powerful tool for detecting the defects on phosphor surfaces, such as electron spin resonance (ESR) analysis, is required. Nevertheless, distinguishing between surface defects, bulk defects, and their entities in small phosphor grains using ESR signals [20] is considerably difficult. We expect that our results will be useful for the surface modification of other UC materials, such as $KBaY(MoO_4)_3$:Yb_{3+}, Er_{3+} and $NaYF_4$:Yb,Er@SiO_2, which are promising candidates for use in optical sensors [21, 22].

4. Conclusion

In this study, to improve the light conversion efficiency of upconversion phosphor, silica nanoparticle-coated $NaYF_4$:(Yb^{3+}, Er^{3+}) microphosphors were prepared by a modified sol–gel method using colloidal silica as a function of concentration. The optimal concentration of colloidal silica was determined by comparing its morphological and optical properties. The $NaYF_4$:(Yb^{3+}, Er^{3+}) phosphor coated with colloidal silica (2.7 wt%) yielded an approximately 9% increase in the PL intensity, as compared with that of the noncoated phosphor, likely because of the suppression of nonradiative recombination via surface defects. The experimental results suggest that the surface coating of phosphors with an appropriate oxide is a simple and effective solution to improve the light conversion efficiency of UCMP phosphors.

Data Availability

All the data used to support the findings of this study are available from the corresponding author upon request.

Conflicts of Interest

The authors declare that there are no conflicts of interest regarding the publication of this paper.

Acknowledgments

This research was supported by the Basic Science Research Program through the National Research Foundation of Korea (NRF), funded by the Ministry of Education (NRF-2019R1I1A3A01041101).

References

[1] M. I. Saleh, B. Rühle, S. Wang, J. Radnik, Y. You, and U. Resch-Genger, "Assessing the protective effects of different surface coatings on $NaYF_4$:Yb^{3+}, Er^{3+} upconverting nanoparticles in buffer and DMEM," *Scientific Reports*, vol. 10, no. 1, pp. 1–11, 2020.

[2] R. G. Geitenbeek, P. T. Prins, W. Albecht, A. van Blaaderen, B. M. Weckhuysen, and A. Meijerink, "NaYF4:Er3+,Yb3+/SiO2Core/Shell upconverting nanocrystals for luminescence thermometry up to 900 K," *Journal of Physical Chemistry C*, vol. 121, no. 6, pp. 3503–3510, 2017.

[3] H. Huang, H. Zhou, J. Zhou et al., "Enhanced anti-stocks luminescence in LaNbO4:Ln3+(Ln3+= Yb3+, Er^{3+}/Ho^{3+}/Tm^{3+}) with abundant color," *RSC Advances*, vol. 7, no. 27, pp. 16777–16786, 2017.

[4] G. Gong, Y. Song, H. Tan et al., "Design of core/active-shell $NaYF_4$:Ln^{3+}@$NaYF_4$:Yb^{3+} nanophosphors with enhanced red-green-blue upconversion luminescence for anti-counterfeiting printing," *Composites Part B: Engineering*, vol. 179, p. 107504, 2019.

[5] A. Dubey, A. K. Soni, A. Kumari, R. Dey, and V. K. Rai, "Enhanced green upconversion emission in $NaYF_4$:Er^{3+}/Yb^{3+}/Li^+ phosphors for optical thermometry," *Journal of Alloys and Compounds*, vol. 693, pp. 194–200, 2017.

[6] J.-C. Boyer and F. C. J. M. van Veggel, "Absolute quantum yield measurements of colloidal $NaYF_4$: Er^{3+}, Yb^{3+} upconverting nanoparticles," *Nanoscale*, vol. 2, no. 8, pp. 1417–1419, 2010.

[7] X. Zhou, X. Xia, B. E. Smith et al., "Interface-dependent radiative lifetimes of Yb^{3+}, $Er3^+$ co-doped single NaYF4 upconversion nanowires," *ACS Applied Materials & Interfaces*, vol. 11, no. 25, pp. 22817–22823, 2019.

[8] C. Homann, L. Krukewitt, F. Frenzel et al., "NaYF4:Yb,Er/NaYF4 core/shell nanocrystals with high upconversion luminescence quantum yield," *Angewandte Chemie International Edition*, vol. 57, no. 28, pp. 8765–8769, 2018.

[9] H. Anwer, J. W. Park, and J.-W. Park, "Near-infrared to visible photon transition by upconverting $NaYF_4$: Yb^{3+}, Gd^{3+}, Tm3+@Bi_2WO_6 core@shell composite for bisphenol A degradation in solar light," *Applied Catalysis B: Environmental*, vol. 243, pp. 438–447, 2019.

[10] F. T. Rabouw, P. T. Prins, P. Villanueva-Delgado, M. Castelijns, R. G. Geitenbeek, and A. Meijerink, "Quenching pathways in NaYF4:Er3+,Yb3+Upconversion Nanocrystals," *ACS Nano*, vol. 12, no. 5, pp. 4812–4823, 2018.

[11] A. A. Vidyakina, I. E. Kolesnikov, N. A. Bogachev et al., "Gd3+-doping effect on upconversion emission of $NaYF_4$: Yb^{3+}, Er^{3+}/Tm^{3+} microparticles," *Materials*, vol. 13, no. 15, p. 3397, 2020.

[12] I. Y. Jung, Y. Cho, S. G. Lee et al., "Optical properties of the $BaMgAl_{10}O_{17}$:Eu^{2+} phosphor coated with SiO_2 for a plasma display panel," *Applied Physics Letters*, vol. 87, no. 19, p. 191908, 2005.

[13] S. H. Sohn, J. H. Lee, and S. M. Lee, "Effects of the surface coating of $BaMgAl_{10}O_{17}$:Eu^{2+} phosphor with SiO_2 nano-particles," *Journal of Luminescence*, vol. 129, no. 5, pp. 478–481, 2009.

[14] J. H. Seo and S. H. Sohn, "Surface modification of the (Y,Gd)BO3:Eu3+ phosphor by dual-coating of oxide nanoparticles," *Materials Letters*, vol. 64, no. 11, pp. 1264–1267, 2010.

[15] W. Deng, L. Sudheendra, J. Zhao et al., "Upconversion in $NaYF_4$:Yb, Er nanoparticles amplified by metal nanostructures," *Nanotechnology*, vol. 22, no. 32, pp. 325604–325612, 2011.

[16] K. L. Reddy, P. K. Sharma, A. Singh et al., "Amine-functionalized, porous silica-coated $NaYF_4$:Yb/Er upconversion nanophosphors for efficient delivery of doxorubicin and curcumin," *Materials Science & Engineering, C*, vol. 96, pp. 86–95, 2019.

[17] G. Arzumanyan, D. Linnik, K. Mamatkulov et al., "Synthesis of NaYF4:Yb,Er@SiO2@Ag core-shell nanoparticles for plasmon-enhanced upconversion luminescence in bio-applications," *Annals of Biomedical Science and Engineering*, vol. 3, pp. 13–18, 2019.

[18] J. Shen, Z. Q. Li, Y. R. Chen et al., "Influence of SiO2 layer thickness on plasmon enhanced upconversion in hybrid Ag/SiO2/NaYF4:Yb, Er, Gd structures," *Applied Surface Science*, vol. 270, pp. 712–717, 2013.

[19] T. Jüstel and H. Nikol, "Optimization of luminescent materials for plasma display panels," *Advanced Materials*, vol. 12, no. 7, pp. 527–530, 2000.

[20] B. S. Chakrabarty, K. V. R. Murthy, and T. R. Joshi, "TSL-EPR correlation study of $LaPO_4$: Ce, Tb," *TÜBİTAK Journal of Physics*, vol. 26, p. 193, 2002.

[21] K. Li, D. Zhu, and H. Lian, "Up-conversion luminescence and optical temperature sensing properties in novel KBaY(MoO4)3:Yb3+,Er3+ materials for temperature sensors," *Journal of Alloy and Compounds*, vol. 816, pp. 152554–152560, 2020.

[22] Z. Li, L. Wang, Z. Wang, X. Liu, and Y. Xiong, "Modification of NaYF4:Yb,Er@SiO_2 nanoparticles with gold nanocrystals for tunable green-to-red upconversion emissions," *Journal of Physical Chemistry C*, vol. 115, no. 8, pp. 3291–3296, 2011.